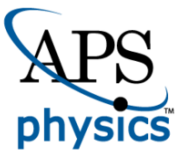

Remnant Geometric Hall Response in a Quantum Quench

Justin H. Wilson, Justin C. W. Song, and Gil Refael

Phys. Rev. Lett. **117**, 235302 — Published 30 November 2016

DOI: 10.1103/PhysRevLett.117.235302

Remnant Hall response in a quantum quench

Justin H. Wilson[1],* Justin C. W. Song[1,2],† and Gil Refael[1,2]
[1] *Institute of Quantum Information and Matter and Department of Physics, and*
[2] *Walter Burke Institute of Theoretical Physics, California Institute of Technology, Pasadena, CA 91125 USA*
(Dated: October 5, 2016)

Out-of-equilibrium systems can host phenomena that transcend the usual restrictions of equilibrium systems. Here we unveil how out-of-equilibrium states, prepared via a quantum quench in a two-band system, can exhibit a non-zero Hall-type current—a remnant Hall response—even when the instantaneous Hamiltonian is time reversal symmetric: a stark contrast with equilibrium Hall currents. Interestingly, the remnant Hall response arises from the coherent dynamics of the wavefunction that retain a remnant of its quantum geometry post-quench, and can be traced to processes beyond linear response. Quenches in two-band Dirac systems are natural venues to realize remnant Hall currents, which exist when *either* mirror or time-reversal symmetry are broken (before or after the quench). Its long time persistence, sensitivity to symmetry breaking, and decoherence-type relaxation processes allow it to be used as a sensitive diagnostic of the complex out-equilibrium dynamics readily controlled and probed in cold-atomic optical lattice experiments.

The subtle quantum coherence encoded in the topology of crystal wavefunctions is responsible for a wide array of robust quantum phenomena [1–4], e.g. the quantum Hall effect. While originating in the solid-state, cold atoms have recently become a system of choice for experimentally unraveling topology on the microscopic level [5–7] due to the array of new probes available. For example, these probes have been used to image the skipping orbits (edge-states) in a cold-atomic quantum Hall system [8], directly measure the Berry curvature [9], and Zak phase [10] in cold-atomic topological bands.

One readily available tool is the *quantum quench*. A state, prepared in the many-body ground state of a Hamiltonian $H(\zeta)$, undergoes a *sudden* change in a physical parameter ζ (e.g. lattice depth, detuning), setting the system into dynamical evolution far from equilibrium [11]. The ease with which distinct Hamiltonians can be accessed via quenches and driving opens up tantalizing possibilities of achieving new out-of-equilibrium phenomena with no equilibrium analog [12–19].

Here we unveil a completely new type of dynamical response achieved in out-of-equilibrium states (OES) which can be prepared via quantum quenches. In particular, we show that certain OES can feature a remnant Hall response even when the instantaneous Hamiltonian preserves time-reversal symmetry (TRS). Remnant Hall responses arise due to the geometric evolution of OES post-quench. Intriguingly, it possesses features such as a Hall current that saturates to a non-zero value at long times (Fig. 1**e**) that have no equilibrium analog.

This can be most easily illustrated for non-interacting and clean Dirac systems, where many-body states can be represented as a collection of pseudospinors on a Bloch sphere (Fig. 1b-d). In these, a state is prepared in the ground state of a Dirac Hamiltonian $H(\Delta)$, with TRS breaking gap Δ (Fig. 1a). At $t = 0$, the Hamiltonian is quenched to $H(\Delta = 0)$ [where TRS is preserved], yielding dynamics for OES, with the pseudospinors exhibiting

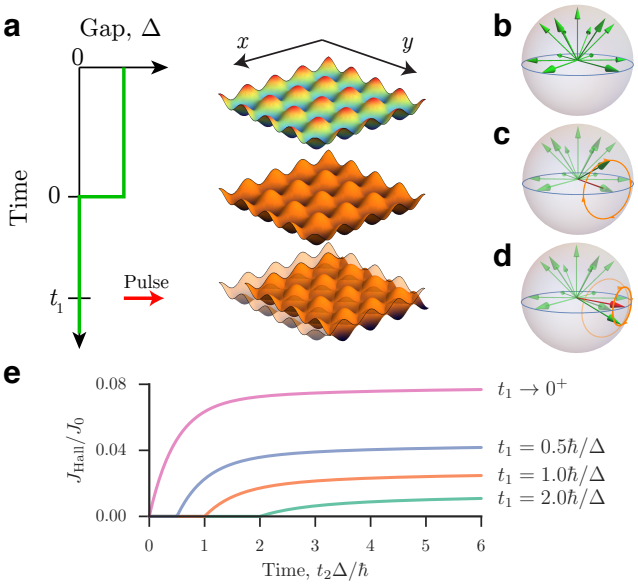

FIG. 1. **a.** Quantum quenches implemented in cold-atomic optical lattices where a parameter in the Hamiltonian is changed suddenly shown by change in color of optical lattice. **b.** Pseudospinors on a Bloch sphere prepared in the Chern insulator state of the Haldane model **c.** exhibit Larmor precession after the Hamiltonian is quenched into zero gap. **d.** The pseudospinors can acquire a transverse shift after the system is pulsed in the longitudinal direction. **e.** Remnant Hall response (orange) for quenching protocol described in Eq. 3 (and panel **b-d**). Here, the green curve shows $\Delta(t)$ quench and characteristic $J_0 = \frac{e^2}{h}\frac{\Delta^2}{e\hbar v_{\rm F}}$.

Larmor precession (Fig. 1c).

To probe OES, a *short* pulse of strength $\mathbf{A} = \int dt\, \mathbf{E}(t)$ can be applied to the system at time $t = t_1$ (Fig. 1**a**,**e**), shifting the Larmor orbits along $\mathbf{E}$. Averaged over one-cycle, longitudinal momentum along $\mathbf{E}$ increases. However, in addition to this, the constraint of pseudospinors being on the Bloch sphere allows a *transverse* shift to

accumulate. As a result, at long times $t = t_2$, we obtain a remnant Hall current

$$\mathbf{J}_{\rm Hall}(t_1, t_2 \to \infty) = \Xi^{\infty}_{\rm Hall}(t_1)\hat{\mathbf{z}} \times \mathbf{A}, \tag{1}$$

that persists long after the pulse $\mathbf{E}(t)$ as shown in Fig. 1e. Here $\Xi^{\infty}_{\rm Hall}$ is non-universal function depending on t_1 and model specifics described below. Instead of the Hall conductivity, we focus on the total current and $\Xi^{\infty}_{\rm Hall}$ because (i) time-translational symmetry is broken and (ii) the effect described here is inherently beyond linear reponse. Additionally, while we use the language of electromagnetic response, in cold-atom optical lattices $e\mathbf{A}$ can be easily effected by a shift in momentum $\Delta\mathbf{p}$ brought on by a sudden force; in such systems $\mathbf{J}_{\rm Hall}$ takes the form of a particle current.

Remnant Hall currents (Eq. (1), Fig. 1**e**) are strikingly different from those found in equilibrium systems in two respects: (1) Without relaxation processes, they persist at infinite times after an applied pulse and (2) involve momentum shifts in the Fermi sea. Therefore, as the Fermi sea relaxes, the Hall current degrades (as would be expected from general considerations [20, 21]).

A useful analogy with the coherent evolution of spins in nuclear magnetic resonance (NMR) protocols can be drawn between real spins and our pseudospins, where decay of the NMR signal can be used as a sensitive diagnostic of scattering, for e.g. spin-spin, spin-environment relaxation. As we argue below, T_2 as a purely dephasing phenomena has *no effect* on the remnant Hall response. However, energy relaxation in the form of T_1 degrades the effect. Therefore, we anticipate that the decay profile of $\mathbf{J}_{\rm Hall}$ that arises from coherent pseudospinor evolution can be used as a diagnostic of relaxation and/or thermalization processes in OES when interactions and disorder are allowed.

The ease with which Dirac-type [9] and other spin-orbit coupled Hamiltonians [5] can be constructed in setups for ultra-cold bosons and fermions allows these effects to be easily accessed—though we find that fermions are more readily amenable. In order to observe the Hall effect and separate it from an overwhelming longitudinal response, we propose a time-of-flight setup in the direction perpendicular to the applied pulse while keeping a confining potential in the direction of the applied pulse. In such an experimental set-up, the gap, as tuned by Zeeman coupling or "shaking" of the cold atom lattice, is suddenly turned off. The "pulse" is then implemented some time after the quench by applying a sudden and brief force upon the system (e.g. tilting the confining potential for a very short time).

Let us now explain the effect with a two-band Hamiltonian $H(\Delta) = \sum_{\mathbf{p}} c^{\dagger}_{\mathbf{p}} h(\mathbf{p}, \Delta) c_{\mathbf{p}}$ with $c_{\mathbf{p}} = (c_{+,\mathbf{p}}, c_{-,\mathbf{p}})^T$ and

$$h(\mathbf{p}, \Delta) = \epsilon_0(\mathbf{p})\mathbb{I} + \mathbf{d}(\mathbf{p}, \Delta(t)) \cdot \boldsymbol{\sigma}, \tag{2}$$

where $\mathbf{p} = (p_x, p_y)$ is the two-dimensional momentum and $\boldsymbol{\sigma} = (\sigma_x, \sigma_y, \sigma_z)$ are the Pauli matrices, and $\Delta(t)$ is a gap parameter that varies as a function of time. When $\mathbf{d}(\mathbf{p}, \Delta(t))$ changes rapidly as in a quantum quench, the response depends intimately on the evolution of the wavefunction.

Before discussing the lattice setup, we first analyze a simple example that captures the essential physics—a quenched, single-cone, low-energy Haldane-type model—obeying Eq. (2) with

$$\epsilon_0(\mathbf{p}) = 0, \quad \mathbf{d}(\mathbf{p}, \Delta(t)) = (p_x, p_y, \Delta\Theta[-t]), \tag{3}$$

where $\Theta(t)$ is the Heaviside function. This captures the essential physics of the usual two-cone Haldane model up to a factor of two, hence the name. For $t < 0$, we begin in the many-body ground state $|\Psi_0\rangle$ at half-filling. For $t > 0$, the system coherently evolves with $|\Psi_1(t)\rangle = e^{-iHt}|\Psi_0\rangle = \prod_{\mathbf{p}} |\psi_1(\mathbf{p})\rangle$ for single particle wave-functions $|\psi_1(\mathbf{p})\rangle = e^{-ih(\mathbf{p},0)t}|\psi_0(\mathbf{p})\rangle$. For this half-filled band, the Chern number (defined by $\mathcal{C} = \int \frac{d^2p}{(2\pi)^2}\hat{\mathbf{z}} \cdot \nabla_{\mathbf{p}} \times \langle\psi_0(\mathbf{p})|i\nabla_{\mathbf{p}}|\psi_0(\mathbf{p})\rangle$) is 1/2 per flavor. In equilibrium, this manifests as a $\sigma_{xy} = \mathcal{C}e^2/h$ bulk Hall conductivity, but as we show, the out-of-equilibrium current response becomes decoupled from the Chern number despite the fact that unitary evolution preserves $\mathcal{C}$ [14, 18].

To extract the response properties of $|\Psi_1(t)\rangle$ we consider the following pulse-type protocol [see Fig. 1] where (i) at $t = t_1$ a short pulse $[E_x(t) = A_x\delta(t - t_1)]$ is applied to the system so that $\mathbf{p} \to \mathbf{p} - e\mathbf{A}$ (i.e. the Hamiltonian in Eq. (3) changes $\mathbf{d}(\mathbf{p}, 0) \to \mathbf{d}(\mathbf{p} - e\mathbf{A}, 0)$), (ii) and the Hall current, $\mathbf{J}_{\rm Hall}$, that develops is measured at $t = t_2$. Here $t_1, t_2 > 0$ occur after the quench leading to a final state $|\Psi_2(t_2)\rangle = \prod_{\mathbf{p}} |\psi_2(\mathbf{p})\rangle$, with $|\psi_2(\mathbf{p})\rangle = e^{-i(t_2-t_1)h(\mathbf{p}-e\mathbf{A},0)}|\psi_1(\mathbf{p}, t_1)\rangle$.

The current response can be obtained via $\mathbf{J} = \langle\Psi|\hat{\jmath}|\Psi\rangle$, where $\hat{\jmath} = \partial H/\partial\mathbf{A}$. Using $|\Psi\rangle = |\Psi_2(t_2)\rangle$ along with Eq. (3) and extracting the component of $\mathbf{J}$ transverse to the applied field $\mathbf{E}$, we obtain $\mathbf{J}_{\rm Hall}$ as shown in Fig. 1e. Here, $\mathbf{J}_{\rm Hall}$ was obtained via numerical integration with a pre-quench $|\Psi_0\rangle$ where the entire valence band was filled. A full discussion of $\mathbf{J}$ is contained in the supplement [22]. Due to the collective action of all electrons in the valence band, $\mathbf{J}_{\rm Hall}$ does not have an apparent oscillatory structure in Fig. 1e.

Strikingly, $\mathbf{J}_{\rm Hall}$ in Fig. 1e grows from zero (when the pulse is first applied at t_1) and saturates at long times to a non-vanishing value, $\mathbf{J}_{\rm Hall}(t_1, t_2 \to \infty) = \mathbf{J}^{\infty}_{\rm Hall}(t_1)$ as seen in Fig. 1e. As we argue below, this behavior is generic for OES. The non-zero $\mathbf{J}^{\infty}_{\rm Hall}(t_1)$ is unconventional and arises from the near-lockstep Larmor precession of the pseudospinors $|\psi_1(\mathbf{p})\rangle$ that form the full many-body OES $|\Psi_1\rangle$.

We can understand this geometrically by considering Larmor precession of the pseudospins on the Bloch

sphere. Even though we are interested in quenches defined in Eq. (3), the following geometric analysis is general and applies to two-band models. Mapping each spinor onto the Bloch sphere via $\hat{\mathbf{n}} = \langle\psi_1(\mathbf{p})|\boldsymbol{\sigma}|\psi_1(\mathbf{p})\rangle$, we can describe the Larmor precession of the spinors via the equations of motion:

$$\partial_t \hat{\mathbf{n}} = 2\mathbf{d}(\mathbf{p},0)\times\hat{\mathbf{n}}, \quad \hat{\mathbf{n}}(t=0) = -\hat{\mathbf{d}}(\mathbf{p},\Delta). \tag{4}$$

To understand *why* this implies a remnant Hall current, consider a ring of momenta with $|\mathbf{p}| = p$ held constant. With Larmor precession for $t > 0$, they will oscillate around a point on the equator, see Fig. 2**a,d**. Then, at time $t = t_1$ we apply a pulse. As shown by the red arrow in Fig. 2b, the pulse has the effect of shifting the center of rotation for Larmor precession $\mathbf{d}(\mathbf{p},0) \to \mathbf{d}(\mathbf{p}-e\mathbf{A},0)$. As a result, at long times the shift in average $\hat{\mathbf{n}}$ persists (see Fig. 2**b,c,e**). Since $\hat{\mathbf{n}}$ directly corresponds to current flow direction in Eq. (3), a remnant Hall current develops.

The long-time average of $\hat{\mathbf{n}}$ is just its projection at time t_1 along the new precession direction $\mathbf{d}(\mathbf{p}-e\mathbf{A},0)$ yielding $[\hat{\mathbf{n}}(t_1)\cdot\hat{\mathbf{d}}(\mathbf{p}-e\mathbf{A},0)]\hat{\mathbf{d}}(\mathbf{p}-e\mathbf{A},0)$. Writing the current operator as $\hat{j}_\mu = -e\partial_{p_\mu} h(\mathbf{p}-e\mathbf{A},0) = -e\partial_{p_\mu}\mathbf{d}(\mathbf{p}-e\mathbf{A},0)\cdot\boldsymbol{\sigma}$, we obtain the current from the projection of the average $\hat{\mathbf{n}}$ along $\partial_{p_\mu}\mathbf{d}(\mathbf{p}-e\mathbf{A},0)$. As a result, the long-time current for a state $\mathbf{p}$ is

$$j_\mu^\infty(\mathbf{p},t_1) = -e[\hat{\mathbf{n}}(\mathbf{p},t_1)\cdot\hat{\mathbf{d}}(\mathbf{p}-e\mathbf{A},0)]\partial_{p_\mu} d(\mathbf{p}-e\mathbf{A},0). \tag{5}$$

The expression in Eq. (5) is independent of a specific two-band model [23].

We now consider the quench specified in Eq. (3) so that $\mathbf{n}(t_1) = \langle\psi_1|\boldsymbol{\sigma}|\psi_1\rangle$ reads as $\mathbf{n}(t_1) = -\mathbf{p}\sin\theta_{\mathbf{p}} + (\cos 2pt_1\,\hat{\mathbf{z}} - \sin 2pt_1\,\hat{\mathbf{z}}\times\hat{\mathbf{p}})\cos\theta_{\mathbf{p}}$ (using $|\psi_1(\mathbf{p})\rangle$ derived earlier). Integrating over all $\mathbf{p}$ (for a filled band prior to quench), we obtain a total current

$$J_\mu^\infty(t_1) = -e\int \frac{d^2p}{(2\pi\hbar)^2}\frac{\hat{\mathbf{n}}(t_1)\cdot(\mathbf{p}-e\mathbf{A})}{|\mathbf{p}-e\mathbf{A}|}\partial_{p_\mu}|\mathbf{p}-e\mathbf{A}|. \tag{6}$$

While this quantity can be fully evaluated (see supplement for discussion), for brevity and to capture the essential physics, we expand Eq. (6) in $\mathbf{A}$. Discarding terms that integrate to zero we arrive at Eq. (1) with $\Xi_{\rm Hall}^\infty(t_1) = -\frac{e^2}{2h}\frac{\Delta}{\hbar}\int_0^{\frac{\pi}{2}} dz\, e^{-2\frac{t_1|\Delta|}{\hbar}\sin z}$.

While $|\psi_1(\mathbf{p})\rangle$ with similar energies precess with frequencies that are close to each other, over long times t_1, small differences in their precession frequency allow their Larmor orbits to slowly drift out of phase, degrading $\mathbf{J}_{\rm Hall}^\infty(t_1)$. Analyzing $J_{\rm Hall}^\infty(t_1)$ for large t_1, we obtain

$$\mathbf{J}_{\rm Hall}^\infty(t_1) = -\,\mathrm{sgn}(\Delta)\frac{e^2}{4h}\frac{A_x}{t_1} + O(t_1^{-2}), \tag{7}$$

which shows that the longer we wait after the quench to pulse the system, the smaller $\mathbf{J}_{\rm Hall}^\infty(t_1)$, as evidenced in the diminishing $\mathbf{J}_{\rm Hall}$ current profiles shown in Fig. 1**e**. This aging behavior is a characteristic of the different energies of the pseudospinors that form pre-quench $|\Psi_0\rangle$.

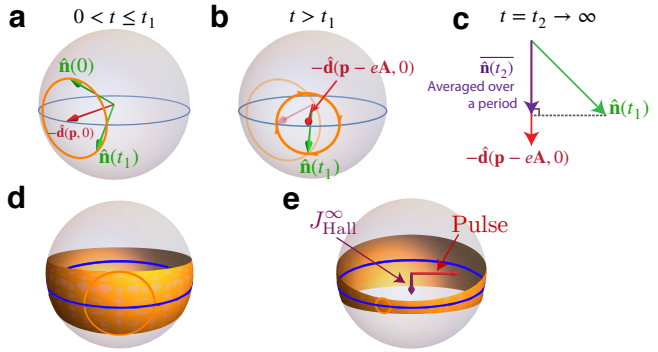

FIG. 2. **a.** After quench, the state $\hat{\mathbf{n}}$ Larmor precesses on the Bloch sphere. **b.** After the pulse, the center of Larmor precession shifts due to the momentum boost $e\mathbf{A}/c$. **c.** For long times, the shift in the state's average over a Larmor period, $\overline{\hat{\mathbf{n}}(t_2)}$, persists leading to a current at $t_2 \to \infty$. **d.** For the Haldane model, Eq. (3), the orange manifold represents the combined Larmor orbits of states with the same $|\mathbf{p}|$. **e.** After the pulse, the manifold of Larmor orbits changes to give a perpendicular shift in the average $\overline{\hat{\mathbf{n}}(t_2)}$ resulting in $J_{\rm Hall}^\infty$.

Importantly, persistent $\mathbf{J}_{\rm Hall}^\infty$ does not occur in equilibrium systems; in fact, it is disallowed since DC conductivity is finite even without disorder. To see this, consider the response in equilibrium captured by $j_y(t) = \int \sigma_{yx}(t-t')E_x(t')dt'$. For a pulse $E_x(t) = A_x\delta(t)$, we have $j_y(t) = \sigma_{yx}(t)A_x$. Thus $\sigma_{yx}^{\rm DC} = \frac{1}{A_x}\int j_y(t)dt$. As a result, for $\sigma_{yx}^{\rm DC}$ that is finite (e.g., the anomalous and conventional Hall effect, the quantum Hall effect), then $j_y(t) \to 0$ as $t \to \infty$ due to integrability.

Relaxation can be included in Eq. (4) in the form of a T_1 and T_2 time [24]. Oscillatory terms describing the Larmor precession are all that are affected by T_2, so if we isolate the non-oscillatory term which gives rise to Eq. (5), we find that only energy relaxation in the form of T_1 time affects the result. In fact, at long times, $j_\mu(\mathrm{p},t_2,t_1) = j_\mu^\infty(\mathbf{p},t_1)e^{-t_2/T_1(p)}$. We expect relaxation processes to occur with a probability roughly determined by Fermi's golden rule such that $1/T_1(p) \sim \gamma\rho[\epsilon(p)]$ where $\rho(\epsilon)$ is the density of states and γ describes the relaxation. In the above model [Eq. (3)], this leads to a suppression as $1/t_2^2$ at long times for $\mathbf{J}_{\rm Hall}$ (see supplement [22]).

OES Hall currents in Eq. (1) depend intimately on the underlying symmetries of the Hamiltonian, h, in Eq. (2). In particular, we find $\Xi_{\rm Hall}^\infty$ depends on the *absence* of either mirror, $M_y^{-1}h(p_x,p_y)M_y = h(p_x,-p_y)$, or time-reversal, $T^{-1}h(-\mathbf{p})T = h(\mathbf{p})$, symmetry. To expose this, we analyze the contribution of $\mathbf{p}$ states to the persistent response in Eq. (5). Expanding in the pulse strength $\mathbf{A}$, we obtain $j_\mu^\infty(\mathbf{p},t_1) \approx \chi_{\mu\nu}^\infty(\mathbf{p},t_1)A_\nu$. Indeed $\Xi_{\rm Hall}^\infty = \int d\mathbf{p}\chi_{\rm Hall}^\infty(\mathbf{p})$, where $\chi_{\rm Hall}^\infty = \frac{1}{2}(\chi_{yx}^\infty - \chi_{xy}^\infty)$. Writing $\mathbf{d}_0 = \mathbf{d}(\mathbf{p},0)$ yields $\chi_{\rm Hall}^\infty = \chi_M^\infty + \chi_T^\infty$, where $\chi_M^\infty =$

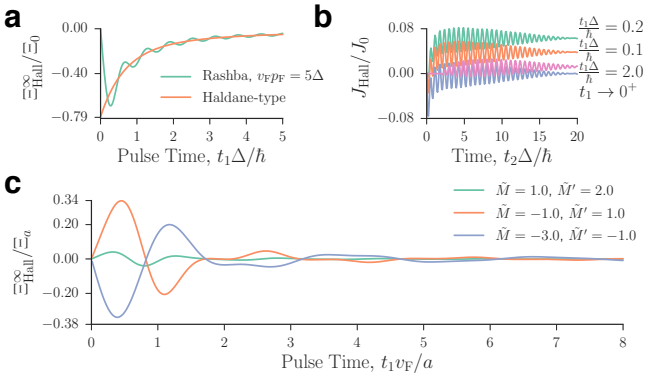

FIG. 3. Other models for OES Hall current. **a.** The long-time persistent $\Xi^{\infty}_{\rm Hall}$ dies off as a function of pulse time t_1 for Haldane and Rashba model. The Fermi momentum cutoff in Rashba causes oscillations and $\Xi_{\rm Hall} \to 0$ as $t_1 \to 0$. **b.** For the Rashba model, the current evolves in an oscillatory way due to the cutoff $p_{\rm F}$. **c.** Persistent $\Xi^{\infty}_{\rm Hall}$ in the half-BHZ model (see text) sees similar oscillations due to the cutoff provided by the square lattice. Interestingly $\Xi^{\infty}_{\rm Hall} \neq 0$, regardless of the phase we begin or end in. For the Rashba model, we used $eA_x = 0.1\Delta/v_{\rm F}$ and $v_{\rm F}p_{\rm F} = 5\Delta$. In the above, characteristic $J_0 = \frac{e^2}{h}\frac{\Delta^2}{e\hbar v_{\rm F}}$, $\Xi_0 = \frac{e^2}{h}\frac{\Delta}{\hbar}$, $\Xi_a = \frac{e^2}{h}\frac{v_{\rm F}}{a}$, and $\tilde{M} = M\frac{a}{\hbar v_{\rm F}}$.

$e^2\partial_{[p_y}d_0\partial_{p_x]}\hat{\mathbf{d}}_0\cdot\hat{\mathbf{d}}\cos 2d_0t_1$, and $\chi^{\infty}_T = -e^2\partial_{[p_y}d_0\partial_{p_x]}\hat{\mathbf{d}}_0\cdot\hat{\mathbf{d}}_0\times\hat{\mathbf{d}}\sin 2d_0t_1$. Here the brackets $\partial_{[p_y}\cdots\partial_{p_x]}$ denote antisymmetrization, and M and T subscripts denote contributions controlled by M_y and T. Importantly, if h possesses M_y-symmetry, then $\chi^{\infty}_M(p_x,p_y) = -\chi^{\infty}_M(p_x,-p_y)$. On the other hand, if h possesses T-symmetry, then $\chi^{\infty}_T(\mathbf{p}) = -\chi^{\infty}_T(-\mathbf{p})$ (see supplement [22]). As a result, when h satisfies both M_y and T symmetries (before and after quench), opposing momentum states will give contributions of opposite sign, and $\Xi^{\infty}_{\rm Hall} = \int d\mathbf{p}\chi^{\infty}_{\rm Hall}(\mathbf{p}) = 0$. Hence, finite $\Xi^{\infty}_{\rm Hall}$ arises from breaking of *either* M_y or T symmetry before or after the quench [25] in contrast to the symmetry requirements for Hall currents in equilibrium linear response [26].

While OES Hall response is disconnected from the Chern number, $\mathcal{C}$, $\Xi^{\infty}_{\rm Hall}$ can still be expressed in terms of bulk band properties. In particular, for M_y symmetric Hamiltonians with a filled band prior to quench, we find an equivalent TKNN-like formula

$$\Xi^{\infty}_{\rm Hall} = -e^2\int\frac{d^2p}{(2\pi)^2}\partial_{t_1}\Omega_{p_yp_x}\log d(\mathbf{p},0), \qquad (8)$$

where $\Omega_{p_yp_x} = \frac{1}{2}\hat{\mathbf{n}}(t_1)\cdot(\partial_{p_y}\hat{\mathbf{n}}(t_1)\times\partial_{p_x}\hat{\mathbf{n}}(t_1))$ is the Berry curvature of the evolved $\mathbf{p}$ state evaluated at pulse time t_1. While arising from Berry curvature, we note that it is manifestly distinct from $\mathcal{C}$ and is not quantized.

Finally, we examine other quench protocols for Eq. (2). As we will see, these yield similar responses to the Haldane protocol examined above. One interesting example is a Rashba type protocol where

$$\epsilon_0(\mathbf{p}) = \frac{p^2}{2m}, \quad \mathbf{d}(\mathbf{p},\Delta) = (-v_{\rm F}p_y, v_{\rm F}p_x, \Delta\Theta(-t)), \quad (9)$$

and chemical potential $\mu = 0$. As shown in Fig. 3a,b, the Rashba protocol also yields a Hall current that persists at long times. Interestingly, the Hall current in Fig. 3a exhibits an oscillatory behavior which arises from the momentum cutoff of Eq. (9) at $p_{\rm F} = v_{\rm F}[2m(mv_{\rm F}^2 + \sqrt{m^2v_{\rm F}^4 + \Delta^2})]^{1/2}$; this contrasts with the smooth behavior of Fig. 1e, which had no momentum cutoff.

For $t_2 \to \infty$, the Hall current response levels out (Fig. 3a,b). Indeed, its persistent response, $\mathbf{J}^{\infty}_{\rm Hall}$, matches the Haldane protocol closely (see Fig. 3a), except in one important way. In the Rashba protocol, it takes a finite t_1 to "turn-on" $\mathbf{J}^{\infty}_{\rm Hall}$: magnitude $\mathbf{J}^{\infty}_{\rm Hall}$ increases from zero at small t_1, and decreases at long t_1. In contrast, the Haldane protocol has maximal $\mathbf{J}^{\infty}_{\rm Hall}$ at $t_1 \to 0^+$. This difference arises due to the momentum cutoff which does not appear in the low-energy model of Eq. (3) where there exist states on the Bloch sphere that have already performed multiple Larmor orbits even for an infinitesimal t_1, yielding a large $\mathbf{J}^{\infty}_{\rm Hall}$.

Quench type protocols exhibiting $\mathbf{J}^{\infty}_{\rm Hall}$ can also be realized in lattice models. In these, the bands are finite as opposed to the continuum bands discussed above. We illustrate such a protocol for a "half-BHZ" type model in a square lattice [27], wherein Eq. (2) takes $\epsilon_0(\mathbf{p}) = 0$ and $\mathbf{d}(\mathbf{p},M(t)) = \frac{\hbar v_{\rm F}}{a}(\sin\frac{ap_x}{\hbar}, \sin\frac{ap_y}{\hbar}, M(t) + 2 - \cos\frac{ap_x}{\hbar} - \cos\frac{ap_y}{\hbar})$. Here $M(t<0) = M$ and $M(t>0) = M'$ represents the quench, and a is the lattice constant. In the ground state, this model has different topological phases represented by M [28] Picking M, M' values allows to quench within and between the trivial and topological phases, yielding a persistent Hall current as well (Fig. 3c). As in the case of the Rashba Hamiltonian, there is "turn-on" behavior with time scale corresponding to the momentum cutoff provided by a^{-1}.

The general framework, as well as the specific model realizations, presented here demonstrate that OES prepared via a quench can manifest Hall currents that persist long after the application of an excitation pulse. Strikingly, they occur under different symmetry requirements than that found in equilibrium systems and can arise even when the instantaneous Hamiltonian is TRS preserving. The experimental conditions necessary for probing OES are readily available in current cold atom setups [29]: the persistent, quench-induced Hall currents described can be measured via time-of-flight and provides a new diagnostic of coherent wavefunction dynamics. The Hall response of OES depend intimately on the entire history of wavefunction evolution unlike in equilibrium. This opens a new vista of unconventional phenomena that can be prepared and probed in OES.

As we were finalizing this manuscript, we became aware of the complementary work of Hu, Zoller, and Budich [30] on out-of-equilibrium Hall responses. They include breaking of translational invariance (by a trap, for instance) and find little effect to the out-of-equilibrium Hall response.

Acknowledgements—We thank Mehrtash Babadi, Eugene Demler, and Ian Spielman for helpful discussions. We thank the Air Force Office for Scientific Research (JW) and the Burke fellowship at Caltech (JCWS) for support. GR is grateful for support through the Institute of Quantum Information and Matter (IQIM), an NSF frontier center, supported by the Gordon and Betty Moore Foundation as well as the Packard Foundation and for the hospitality of the Aspen Center for Physics, where part of the work was performed.

* jwilson@caltech.edu
† justinsong@ntu.edu.sg

[1] Klaus Von Klitzing, "The quantized Hall effect," Rev. Mod. Phys. **58**, 519–531 (1986).
[2] Naoto Nagaosa, Jairo Sinova, Shigeki Onoda, A. H. MacDonald, and N. P. Ong, "Anomalous Hall effect," Rev. Mod. Phys. **82**, 1539–1592 (2010).
[3] Horst L. Stormer, Daniel C. Tsui, and Arthur C. Gossard, "The fractional quantum Hall effect," Rev. Mod. Phys. **71**, S298–S305 (1999).
[4] K. V. Klitzing, G. Dorda, and M. Pepper, "New method for high-accuracy determination of the fine-structure constant based on quantized hall resistance," Phys. Rev. Lett. **45**, 494–497 (1980).
[5] Y.-J. Lin, K. Jiménez-García, and I. B. Spielman, "Spin–orbit-coupled Bose–Einstein condensates," Nature **471**, 83–86 (2011).
[6] Immanuel Bloch, Jean Dalibard, and Sylvain Nascimbène, "Quantum simulations with ultracold quantum gases," Nature Phys. **8**, 267–276 (2012).
[7] Sebastian Will, Deepak Iyer, and Marcos Rigol, "Observation of coherent quench dynamics in a metallic many-body state of fermions," Nature Commun. **6**, 6009 (2015).
[8] B. K. Stuhl, H. I Lu, L. M. Aycock, D. Genkina, and I. B. Spielman, "Visualizing edge states with an atomic Bose gas in the quantum Hall regime," Science **349**, 1514–1518 (2015).
[9] Gregor Jotzu, Michael Messer, Rémi Desbuquois, Martin Lebrat, Thomas Uehlinger, Daniel Greif, and Tilman Esslinger, "Experimental realization of the topological Haldane model with ultracold fermions," Nature **515**, 237–240 (2014).
[10] Marcos Atala, Monika Aidelsburger, Julio T. Barreiro, Dmitry Abanin, Takuya Kitagawa, Eugene Demler, and Immanuel Bloch, "Direct measurement of the Zak phase in topological Bloch bands," Nature Physics **9**, 795–800 (2013).
[11] Markus Greiner, Olaf Mandel, Theodor W Hänsch, and Immanuel Bloch, "Collapse and revival of the matter wave field of a Bose-Einstein condensate." Nature **419**, 51–54 (2002).
[12] Takashi Oka and Hideo Aoki, "Photovoltaic Hall effect in graphene," Phys. Rev. B **79**, 081406(R) (2009).
[13] Takuya Kitagawa, Takashi Oka, Arne Brataas, Liang Fu, and Eugene Demler, "Transport properties of nonequilibrium systems under the application of light: Photoinduced quantum Hall insulators without Landau levels," Phys. Rev. B **84**, 235108 (2011).
[14] Luca D'Alessio and Marcos Rigol, "Dynamical preparation of Floquet Chern insulators," Nature Commun. **6**, 8336 (2015).
[15] Mark S. Rudner, Netanel H. Lindner, Erez Berg, and Michael Levin, "Anomalous edge states and the bulk-edge correspondence for periodically driven two-dimensional systems," Phys. Rev. X **3**, 031005 (2013).
[16] L. E F Foa Torres, P. M. Perez-Piskunow, C. A. Balseiro, and Gonzalo Usaj, "Multiterminal conductance of a floquet topological insulator," Phys. Rev. Lett. **113**, 266801 (2014).
[17] Jan Carl Budich and Markus Heyl, "Dynamical topological order parameters far from equilibrium," (2015), arXiv:1504.05599.
[18] M D Caio, Nigel R. Cooper, and M J Bhaseen, "Quantum Quenches in Chern Insulators," Phys. Rev. Lett. **115**, 236403 (2015).
[19] Hossein Dehghani, Takashi Oka, and Aditi Mitra, "Out-of-equilibrium electrons and the Hall conductance of a Floquet topological insulator," Phys. Rev. B **91**, 155422 (2015).
[20] Michael Stark and Marcus Kollar, "Kinetic description of thermalization dynamics in weakly interacting quantum systems," (2013), arXiv:1308.1610.
[21] Bruno Bertini and Maurizio Fagotti, "Pre-relaxation in weakly interacting models," J. Stat. Mech. Theory Exp. **07012**, P07012 (2015), arXiv:1501.07260.
[22] See Supplemental Material at [URL will be inserted by publisher] for calculational details.
[23] A two-band model neglecting current contributions from $\epsilon_0(\mathbf{p})$; however, those contributions do not have a Hall response.
[24] Dmitry Budker, Dererk F Kimball, and David P DeMille, *Atomic Physics: An Exploration through Problems and Solutions* (Oxford University Press, 2008).
[25] Indeed, h in Eq. 3 possesses M_y symmetry (anti-unitary symmetry), but $h(t<0)$ breaks T symmetry resulting in the observed Hall current.
[26] Inti Sodemann and Liang Fu, "Quantum Nonlinear Hall Effect Induced by Berry Curvature Dipole in Time-Reversal Invariant Materials," Phys. Rev. Lett. **115**, 216806 (2015).
[27] B. Andrei Bernevig and Taylor L. Hughes, *Princeton University Press* (Princeton University Press, 2013) p. 264.
[28] $M>0$ and $M<-4$ are trivial with equilibrium $\sigma_{xy}=0$, $-2<M<0$ is a topological insulator with equilibrium $\sigma_{xy}=-1$, and $-4<M<-2$ is also a topological insulator with equilibrium $\sigma_{xy}=+1$.
[29] Dan M. Stamper-Kurn and Masahito Ueda, "Spinor Bose gases: Symmetries, magnetism, and quantum dynamics," Rev. Mod. Phys. **85**, 1191–1244 (2013).
[30] Ying Hu, Peter Zoller, and Jan Carl Budich, "Dynamical Buildup of a Quantized Hall Response from Non-Topological States," (2016), arXiv:1603.00513.